UC Irvine
UC Irvine Previously Published Works

Title

Integrated platform for functional monitoring of biomimetic heart sheets derived from human pluripotent stem cells.

Permalink

https://escholarship.org/uc/item/1816c2x9

Journal

Clinical materials, 35(2)

Authors

Chen, Aaron

Lee, Eugene

Tu, Roger

et al.

Publication Date

2014

DOI

10.1016/j.biomaterials.2013.10.007

Peer reviewed

eScholarship.org Powered by the California Digital Library
University of California

Author Manuscript

Author Manuscript

Author Manuscript

Author Manuscript

HHS Public Access

Author manuscript

Biomaterials. Author manuscript; available in PMC 2022 July 21.

Published in final edited form as:

Biomaterials. 2014 January ; 35(2): 675–683. doi:10.1016/j.biomaterials.2013.10.007.

Integrated platform for functional monitoring of biomimetic heart sheets derived from human pluripotent stem cells

Aaron Chen[a,1], **Eugene Lee**[b,1], **Roger Tu**[c], **Kevin Santiago**[b], **Anna Grosberg**[b], **Charless Fowlkes**[b,d], **Michelle Khine**[a,b,*]

[a] Department of Chemical Engineering and Materials Science, University of California, Irvine, CA, USA

[b] Department of Biomedical Engineering, University of California, Irvine, CA, USA

[c] Department of Biological Sciences, University of California, Irvine, CA, USA

[d] Department of Computer Science, University of California, Irvine, CA, USA

Abstract

We present an integrated platform comprised of a biomimetic substrate and physiologically aligned human pluripotent stem cell-derived cardiomyocytes (CMs) with optical detection and algorithms to monitor subtle changes in cardiac properties under various conditions. In the native heart, anisotropic tissue structures facilitate important concerted mechanical contraction and electrical propagation. To recapitulate the architecture necessary for a physiologically accurate heart response, we have developed a simple way to create large areas of aligned CMs with improved functional properties using shrink-wrap film. Combined with simple bright field imaging, obviating the need for fluorescent labels or beads, we quantify and analyze key cardiac contractile parameters. To evaluate the performance capabilities of this platform, the effects of two drugs, E-4031 and isoprenaline, were examined. Cardiac cells supplemented with E-4031 exhibited an increase in contractile duration exclusively due to prolonged relaxation peak. Notably, cells aligned on the biomimetic platform responded detectably down to a dosage of 3 nM E-4031, which is lower than the IC_{50} in the hERG channel assay. Cells supplemented with isoprenaline exhibited increased contractile frequency and acceleration. Interestingly, cells grown on the biomimetic substrate were more responsive to isoprenaline than those grown on the two control surfaces, suggesting topography may help induce more mature ion channel development. This simple and low-cost platform could thus be a powerful tool for longitudinal assays as well as an effective tool for drug screening and basic cardiac research.

Keywords

Human pluripotent stem cells; Cardiomyocytes; Drug screening; Contractile properties

* Corresponding author. Department of Biomedical Engineering, University of California, Irvine, 3113 Natural Sciences II, CA 92697, USA. Tel.: +1 949 824 4051; fax: +1 949 824 1727. mkhine@uci.edu (M. Khine).

[1] Equal contribution.

Appendix A. Supplementary data

Supplementary data related to this article can be found online at http://dx.doi.org/10.1016/j.biomaterials.2013.10.007.

Author Manuscript Author Manuscript Author Manuscript Author Manuscript

1. Introduction

Drug attrition is one of the major contributing factors to the high development costs for drugs, especially at later phases of clinical trials. Drug safety, toxicity, and efficacy contributed to 60% of drug attrition in 2000 [1]. Among drug safety issues, drug-induced cardiotoxicity accounted for more than 30% of withdrawals [2]. Numerous Food and Drug Administration (FDA) approved drugs, such as tegaserod and sibutramine, have been withdrawn in the years following their initial approval due to cardiotoxicity concerns. The ineffectiveness of current drug screening methods in the preclinical and clinical phases to detect cardiotoxicity puts patients' health in unnecessary risk. Although animal studies are performed in preclinical trials to screen for cardiotoxicity, the electrophysiological and mechanical properties of human cardiomyocytes are significantly different from those of animals. Therefore, results from these animal studies are notoriously unpredictive with regards to both toxicity and efficacy of drugs [3]. In order to reduce late stage drug attrition associated with cardiotoxicity, decrease drug development costs and ensure patient safety, the development of a biomimetic drug screening platform for the early detection of cardiotoxicity is essential.

With advancements in human pluripotent stem cell (hPSC) research, the ability to yield cardiomyocytes (CMs) [4–6] for *in vitro* models for drug discovery and toxicity screens as well as injury repair have been demonstrated [7–10]. However, properties of hPSC-CMs from current differentiation and culture methods are still significantly different than those of adult CMs. Unlike adult CMs, hPSC-CMs typically exhibit embryonic-like phenotypes and physiology such as immature structural developments [11], electrophysiological functions [12], and weak contractile forces compared to their adult counterparts. Such differences can cause dissimilar cellular responses to drug compounds when compared to those of the native myocardium. Furthermore, currently available cell-based drug and toxicity screens typically work with arrayed single cells or randomized 2-D planar cultures, neither of which recapitulates the physiological constraints and boundary conditions necessary for a physiologically accurate heart response [13,14]. This lack of proper mechanical structure prevents the cells from physiologically relevant responses. To improve current platforms' efficacy as a myocardial model for drug screening, the hPSC-CMs need to be cultured where the cells have physical and electrophysiological attributes akin to those of native heart tissue.

Conventional hPSC-CM culture and tissue engineering methods do not provide the native micro-environmental factors and cues that induce proper maturation, development, and tissue-level behavior [13]. In the native myocardium environment, CMs are naturally aligned. This organization facilitates important mechanical contraction and electrical propagation. It has been shown that the alignment of CMs induce the alignment of sarcomere structures, anisotropic action potential propagations, and higher contractile forces [15]. Previous studies on the effects of structural organization on myocardium have utilized traditional microfabrication techniques such as photolithography [14,16]. These techniques produce homogenous and repetitive patterns not representative of *in vivo* structuring. Furthermore, these techniques are not compatible with scalable large area manufacturing. While the surface abrasion technique is fast and cheap, it cannot produce the multi-scaled, self-similar bundle-like surface topographies and lacks controllability and

Author Manuscript Author Manuscript Author Manuscript Author Manuscript

tunability [17,18]. The surfaces created by these conventional fabrication processes are not representative of the underlying extra cellular matrix (ECM) fibrils in the native heart. We have previously demonstrated that a wrinkled substrate derived from plasma treated pre-stressed thermoplastic shrink film can potentially serve as an efficacious biomimetic surface to functionally align hPSC-CMs and prevent re-entry of ventricular arrhythmia [19,20].

Several methods have been established for characterizing CMs. Electrophysiological properties are often measured through the use of patch clamps [21] or fluorescent voltage sensitive dyes [19,20] which typically serve as end-point assays. With the prohibitive cost and limited supply of hPSC-CMs, invasive characterization assays are undesirable. While there are setups for high-throughput measurements [22], these methods typically provide less content. Several non-invasive, bright field based, characterization techniques have recently been proposed. Many of these techniques utilize optical microscopy combined with image analysis. These image analysis techniques incorporate various algorithms based on fast Fourier transform [23], light intensity changes [24], or motion vectors [25]. The cellular resolution ranges from single cell to confluent cardiac monolayer. However, there appears to be limitations on the CM characterization variables that can be extracted from the frequency and intensity based algorithms. It has been shown that motion vector analysis can be used to track simple contractile occurrences in neonatal rat CMs. However, such current motion vector analysis primarily incorporates average motion vector distances (amplitudes) without regard to the directionality of the vectors; importantly, this results in loss of temporal and spatial information. In more complex and irregular contractile patterns, such as tachycardia, analyses relying solely on average motion vector distances are ineffective as the amplitudes representing cells contracting and relaxing overlap. In fact, we demonstrate that under certain conditions, multiple peaks can be embedded within a single peak in an average motion vector displacement trace (Fig. 3A). To resolve the overlapped peaks, expensive high-speed cameras are often required [25]. However, a CM contractile analysis that utilizes motion vectors should incorporate both the direction and magnitude of the vectors to achieve higher accuracy and more detailed information without the need for a high-speed camera setup.

Leveraging our biomimetic wrinkled substrate [19], we have developed a non-invasive configurable cardiac characterization and drug screen platform based on image correlation analysis [26,27]. Using custom in-house software, this non-invasive platform does not require expensive equipment such as a high-speed camera or fluorescent microscope, and can determine important cardiac contractile properties. We hypothesize that the hPSC-CMs aligned on the biomimetic wrinkles will behave physiologically more similar to functional CMs, when compared to those of randomly organized cells or those aligned by homogenous lines. Furthermore, the effects of two drug compounds on the functional parameters of the CMs are tested to determine the efficacy of this platform.

Author Manuscript Author Manuscript Author Manuscript Author Manuscript

2. Materials and methods

2.1. Cell culture substrate fabrications

To create stamp molds, polydimethylsiloxane (PDMS) (Sylgard 184; Dow Corning Corporation, Midland, MI) monomer and curing agent are initially mixed at a 1:10 ratio. The mixture is then degassed by centrifuging at 3000 rpm for 5 min. Hot embossed substrates involve the fabrication of the desired pattern and pouring PDMS over the given pattern in a 60 mm dish. The dish is vacuumed overnight and cured in an oven at 72 °C for a minimum of 5 h. With the PDMS stamp being cut out, polystyrene (PS) (Grafix Clear Shrink Film, Grafix, Maple Heights, OH) sheets are placed atop the featured side, and together as a whole are sandwiched by glass slides. The set up is heated at 150 °C for 30 min. Features on the PDMS stamp will be hot embossed and transferred onto the PS sheet.

To fabricate the flat substrate, a piece of PS sheet is trimmed and mounted onto a 15 mm circular glass coverslip. For wrinkled substrates, wrinkled PDMS stamps are fabricated and hot embossed into PS sheets before mounting to the glass coverslip. To create this PDMS stamp, pre-stressed polyethylene (PE) shrink-film (Cryovac® D-film, LD935, Sealed Air Corporation) is treated with oxygen plasma (Plasma Prep II, SPI Supplies) for 15 min. The film is shrunk uniaxially in an oven at 150 °C for 3 min. The resulting wrinkled PE is then used as a master mold for creating the negative wrinkled PDMS stamp used for hot embossing PS.

Similar to the wrinkled substrates, the line substrates, with 8 μm width, are produced by hot embossing the lined features into a PS sheet mounted onto circular glass coverslips. However, the fabrication of a 8-μm line stamp involves the use of photolithography. A silicon wafer (4″, Polishing Corp., Santa Clara, California, USA) is initially cleaned and dehydrated overnight on a hotplate. The SU-8 (MicroChem corp., Massachusetts, USA) is then spun onto the wafer for 5 s at 500 rpm and again for 30 s at 1000 rpm. The wafer is soft baked for 3 min at 65 °C or 5 min at 95 °C respectively. An 8-μm mask, produced by Fine Line Imaging (Fine Line Imaging, Colorado Springs, Colorado, USA), is fixed onto the wafer, sandwiched by glass and placed in the DUV flood hood for 15 s. The wafer is developed in a wash dish with SU-8 developer for 3 min, washed with IPA and dried with compressed air. The PDMS is then poured onto the wafer to create the negative 8-μm stamp.

The cell culture substrates are finally sterilized by submerging them in 95% ethanol and then treating them with UV light for at least 30 min.

2.2. Cell cultures and cardiac differentiation

Feeder-free H9 human embryonic stem cells (hESCs) transduced with both αMHC-mCherry-Rex-Bla^r and αMHC-Puro^r-Rex-Neo^r constructs are used, courtesy of the Mercola lab [28]. These cells are cultured on tissue culture plates coated with 1:200 Matrigel® (BD Biosciences, San Jose, California, USA). The cells are fed daily with mTeSR1 medium (StemCell Technologies, Vancouver, Canada). Cells are passaged when they reach 80–90% confluence. To induce cardiac differentiation, the medium is changed to RPMI-B27 (without insulin) (Life Technologies, Grand Island, New York, USA) with a supplement of 100 ng/ml activin A (R&D Systems, Minneapolis, Minnesota, USA) for the first 24 h. Afterwards, the

Author Manuscript Author Manuscript Author Manuscript Author Manuscript

medium is exchanged and incubated with fresh RPMI-B27 (without insulin) supplemented with BMP4 (10 ng/ml) for 4 additional days. On day 5, medium is replaced with the RPMI-B27 (with insulin) again, but without any supplementary cytokines. The medium is exchanged every 2–3 days hereafter [4]. Spontaneous contractions are typically observed on differentiation day 9. hESC-CMs are purified by adding 1.8 μg/mL of puromycin (Life Technologies, Grand Island, New York, USA) in the culture medium on day 20 for 2 days. Cells are rinsed with DPBS twice, and are allowed to recover from the selection process for at least 3 days prior to experiments.

2.3. Drug treatment

E-4031 and isoprenaline (SigmaAldrich, St Louis, Missouri, USA) are added to the culture at a cumulative concentration of 0, 1, 3, 10, and 30 nM, and 0, 0.1, 1, 10, and 100 nM, respectively. At each drug concentration, cells were allowed to incubate for 30 min before imaging. Live time-lapse imaging is described in the following section. After imaging, an additional amount of the drug is added such that the total concentration in the culture is equal to the next target concentration. At the end of experiment, cells are fixed and stained for alignment analysis (Supplementary Information).

2.4. Time-lapse imaging

Images of contracting cardiomyocytes were taken using a Nikon TE 300 (Nikon, New York, USA) inverted microscope equipped with fluorescent optics. Bright field and fluorescent images are taken with a QIClick CCD camera using Q Capture software (Q Imaging, Canada). For live cell imaging, temperature and pH were controlled by the bipolar temperature controller (model TC-202A) connected to an open perfusion microincubator (Harvard Apparatus, Massachusetts, United States). Images were taken at 7 fps for the isoprenaline experiments at a resolution of 1392 × 1040, and were taken at 20 fps for the E-4031 experiments at a resolution of 696 × 520.

2.5. Data processing and analysis for contraction properties

Once the optical flow (OF) analysis (Supplementary Information) is completed and a matrix containing the x- and y-directional vectors are generated, an in-house MATLAB script that calculates the duration, frequency, synchronicity, orientation, and acceleration of cell contractions is applied. To begin this post optical flow contraction (pOFC) analysis, the user will need to input a noise threshold, degree of error, time interval, and starting frame number into the guided user interface. The noise threshold refers to the cutoff value; if the maximum value in the grid of cells is below the cutoff, it is considered to be noise, and is assigned a value of zero. The degree of error represents the flexibility in determining the stage of a contraction (i.e. contraction vs. relaxation) (Supplementary Fig. 1A). The time interval is the time between each consecutive frame. The starting frame number allows user to eliminate partial contractions.

After the inputs have been submitted, the software calculates the occurrences of contraction and relaxation in each individual grid for the entire movie duration. Instead of the magnitude values, categorical variables are used when determining the number of contraction and relaxation occurrences in each grid. The cells within the grids are either contracting

Author Manuscript Author Manuscript Author Manuscript Author Manuscript

(represented by a value of 1), relaxing (a value of −1), or at rest (a value of 0). To determine when cells are at rest, a resting threshold is calculated for each individual grid using the following equation: Resting Threshold = Minimum Trough + 0.25 × (Maximum Peak – Minimum Trough). If the magnitude vector for a given time frame in a grid is below the resting threshold, then the cells within that grid for that specific time frame are deemed at rest. With the input of the starting frame number, the software searches for the first sign of a contraction and assigns the grid a value of 1 for that time frame. The vector direction of the same grid in subsequent time intervals is then compared to the previous time interval. If the direction of the vector is opposite of that in the previous frame and within the degree of error, and has a magnitude value above resting threshold, the cells in the grid are identified as in the relaxing stage, a value of −1.

A complete occurrence is defined as a contraction, relaxation and resting phase in sequence in a grid. If a grid does not have a complete occurrence throughout the time span, then the grid is deemed insignificant and not considered in any of the calculations. After the software converts all grids into categorical values and filters out insignificant grids, the average duration and average frequency of each grid is calculated. The frequency is defined as the number of complete occurrences per second (Supplementary Fig. 1B). The duration of a complete occurrence is defined as the time between the first time interval where contraction occurs and the last time interval that exhibits relaxation. The software measures synchronicity among the occurrences of grids with the phase difference analysis. This analysis is done by taking the most popular pattern of occurrences and calculating the difference between this pattern and all the other patterns. The orientation of the grids is measured by computing the ratio between the sum of magnitude of all y-directional vectors and the sum of magnitude of all x-directional vectors over all time frames. The software also determines the acceleration of each grid by calculating the change of displacement over the change of time.

2.6. Statistics

All contraction analyses are conducted in three independent experiments ($n = 3$ for each type of substrate). Within each substrate at each time point, 5 fields of views are captured per experiment. All bar graphs are reported as MEAN ± S.D. Lilliefors' test for normality was performed to determine distribution of data. Two-tailed Student's *t*-test with unequal variance was used for calculating statistical significance between treatments (Microsoft Excel, Redmond, WA).

3. Results

3.1. Cell alignment on various topographies

Alignment efficiency was evaluated on flat, line, and wrinkled substrates using mouse embryonic fibroblasts (MEFs) and hESC-CMs. Alignment was defined as the percent of f-actin aligned to within ±15° to the direction parallel to the line or wrinkled patterns. For MEFs, 19 ± 5, 41 ± 6, and 51 ± 4% of cells aligned on flat, line, and wrinkled substrates, respectively, after 24 h of the initial plating (Supplementary Fig. 3). The alignment efficiency of MEFs grown on the wrinkles was about 23% higher than that of the line.

Author Manuscript Author Manuscript Author Manuscript Author Manuscript

For hESC-CMs, 20 ± 2, 35 ± 0.5, and 42 ± 1% of cells aligned on flat, line, and wrinkled substrates, respectively, after 24 h (Fig. 1). The alignment efficiency of hESC-CMs grown on the wrinkles was about 20% higher than those grown on the line. In addition to f-actin, sarcomeres were also aligned to the direction of the line and wrinkles as demonstrated by the orientational order parameters (OOP) [15]. For OOP, a value of 0 represents a complete randomized organization, and a value of 1 represents a perfect organization of structures. For hESC-CMs, the OOPs were 0.06 ± 0.01, 0.17 ± 0.02, and 0.25 ± 0.02 for cells aligned on flat, line, and wrinkled substrates, respectively, after 24 h (Fig. 1). The OOP of the hESC-CMs cultured on the wrinkled substrates is close to the OOP measured in primary cardiomyocytes (~0.35) cultured on anisotropic fibronectin patterns [29].

3.2. Evaluation of post optical flow contraction analysis (pOFC)

After the motion vectors were created by the OF analysis, the pOFC analysis was applied to determine various cardiac contractile properties. A series of images was first divided into several grids, and the size of the grids was user defined (Fig. 2A). The contractile properties could be analyzed individually for each grid, or, collectively as an entire image. Based on the displacements, or amplitudes, of the motion vectors, traces of contractions were generated (Fig. 2B, green trace). A full contraction was defined as a sequence of contraction and relaxation of the cardiac cells. Therefore, each full contraction consists of two peaks. However, under arrhythmic conditions, multiple peaks could have been embedded under a single peak (Fig. 3A). The embedded peaks were not resolvable by simply analyzing the contractile displacements, and if unaddressed, could negatively impact the analysis. To attend to this problem, the directions of the motion vectors were also considered for analyzing the contractile properties (Fig. 2B, red trace). Since the directions of motion vectors are approximately opposite to each other during contraction and relaxation, the embedded peaks could be decoupled and displayed in a categorical plot. Based on the categorical plots of each grid, the average contractile duration, frequency, synchronicity, orientation, and acceleration were extracted (Fig. 2C).

To evaluate the accuracy of pOFC analysis code, several slow contracting hESC-CM colonies were imaged at differentiation day 60, and analyzed by visual and automatic inspections. The average contractile duration was 1.16 ± 0.06 and 1.13 ± 0.03 s, and the frequency was 0.57 ± 0.02 and 0.59 ± 0.03 Hz ($n = 5$) for manual and auto analysis, respectively ($p \sim 0.45$ for both cases). The contractile orientation was determined by breaking down the motion vectors into x and y components. In this study, all images of aligned cells were taken with the direction of alignment parallel to the *y*-axis. Therefore, aligned cells are expected to have larger displacements in the *y*-direction than those in the *x*-direction. As expected, the orientation value for cells grown on the flat, line, and wrinkled surfaces were 0.97 ± 0.06, 1.21 ± 0.23, and 1.73 ± 0.16, respectively ($n = 5$).

To examine the code's capability of determining synchronicity as well as its effectiveness of the phase plot difference analysis, a stack of modified images with a predetermined difference in synchronicity was evaluated. To create this stack, the original image of hESC-CMs on a flat surface at 40x magnification was cropped such that the left half of the image remained. The left half was then replicated, placed to right side of the cropped image,

Author Manuscript Author Manuscript Author Manuscript Author Manuscript

and merged. To create a predetermined difference in synchronicity, the right half of the merged image remained unchanged for 5 time frame intervals, while the left half progressed normally. The intention of this image modification was to identify whether or not the code could pick up the differences in synchronicity between two identical contracting CM colonies that are offset by 5 frame intervals. After the modified image stack was processed, it was shown that the two most common occurring bins were 0 and 5 time frames (423 and 385 occurrences respectively). This suggests that the code was able to detect the imposed 5 time frame interval delay on the right side of the image (Supplementary Fig. 6).

3.3. Effect of drugs on cardiac contractions

To evaluate the effectiveness of this integrated functional monitoring platform of biomimetic cardiac sheet for drug screening, the effects of known and well-established proarrhythmic compounds, E-4031 and isoprenaline, were examined. Cardiac cells grown on all three surfaces (flat, lines, and wrinkles) were subjected to these drugs at various concentrations, and different contractile parameters were evaluated. The experiments were done in three replicates for each condition.

E-4031, a specific inhibitor of I_{Kr}, was introduced to the cardiac cultures at increasing concentrations of 0, 1, 3, 10, and 30 nM. The experiments were conducted using cells around differentiation day 40. The cardiac cells did not respond to 1 nM of E-4031 regardless of the type of the culture substrates used. However, the contractile duration significantly increased by 55% at both 10 and 30 nM, and the orientation decreased by 45% at 3 nM and further dropped to about 50% at both 10 and 30 nM for cells grown on the wrinkles (Fig. 3B, bar graph). The increase in contractile duration was exclusively due to the broadened relaxation peak and prolonged relaxation process (Fig. 3B, line graph). The amplitude of the broadened relaxation peak was about 50% compared to that of the control (0 nM). Additionally, the shape of the contraction peaks were almost unaffected by the drug between the control and 30 nM condition. The contractile synchronicity was unchanged in all cases (data not shown).

Isoprenaline, a β-adrenergic agonist, was introduced to the cardiac cultures at increasing concentrations of 0, 0.1, 1, 10, and 100 nM. Three cardiac cell ages were evaluated around differentiation days 20, 40, and 60 for trials 1, 2, and 3, respectively. Despite different cell ages, positive chronotropic effect of isoprenaline was observed from all conditions. In addition, the motion vector displacement analysis revealed the irregular beating patterns as the drug concentration increased for the cells grown on the wrinkles (Fig. 3A). Corroborating with the displacement data, the pOFC analysis additionally revealed a positive inotropic effect. An increasing in contractile frequency (162, 144, and 144% for flat, lines, and wrinkles, respectively) and acceleration (173, 139, 209% for flat, lines, and wrinkles, respectively) was observed for cells grown on all three surfaces when compared between 0 and 100 nM conditions (Fig. 4, table). The contractile synchronicity (100, 108, and 74% for flat, lines, and wrinkles, respectively) and orientation (98, 94, and 78% for flat, lines, and wrinkles, respectively) decreased for cells grown on the wrinkles, and remained relatively unchanged for cells grown on the flat and line surfaces. The contractile duration

Author Manuscript Author Manuscript Author Manuscript Author Manuscript

decreased for cells grown on the flat (76%) and wrinkled (63%) surfaces, but, was relatively unchanged (104%) for those grown on the lined surface.

4. Discussion

As described in the previous sections, three different culture substrates were evaluated: flat, lines, and wrinkled surfaces. The substrates were all made from the same cell culture compatible PS, and the surfaces were oxidized by UVO treatment prior to ECM coating. However, the substrate material is not limited to PS. The wrinkled pattern can be hot embossed into almost any type of plastics as well as transferred onto PDMS; this makes it a versatile platform which can be integrated into other technologies such as the muscular thin film (MTF) for measurement of contractile force [15]. The line substrates have a repetitive pattern of 8 μm width and 2 μm depths. The width of the line was chosen to be in the same range of those which induced strong alignment and elongation of neonatal rat CMs [18]. The initial mold of the line substrate was fabricated using traditional photolithographic methods; thus, the line substrates functioned as an additional control to compare the cellular behaviors to those grown on the wrinkles. As previously described, the biomimetic wrinkled substrates have wrinkle patterns that are self-similar and multiscale with wavelengths ranging from 50 nm to 3 μm [19]. The differences of cellular responses between nano- and microcues have been discussed elsewhere [14]. Previously, we have demonstrated that the shape of action potential propagation of hESC-CMs grown on the wrinkles was anisotropic with an aspect ratio of 2.0 (longitudinal/transverse directions) similar to those in native ventricles [30,31], and the occurrence of both spontaneous and inducible arrhythmias was reduced by 65% [20]. In this study, cardiac cells grown on the wrinkles demonstrated the best alignment in both f-actin and α-actinin when compared to those grown on the flat and lines (Fig. 1B). The contractile orientation of cardiac cells without the addition of drugs further corroborated the alignment efficiency of the wrinkled substrate. In every trial, the cells grown on the flat did not exhibit any preferred contractile orientation between x and y directions; whereas, the cells grown on the lines and wrinkles had preferred orientation parallel to the direction of the patterns. Furthermore, the orientation values of those from the wrinkles were significantly higher than those from the lines (Fig. 4, Supplementary Figs. 7 and 8). These results indicate that optical microscopy combined with pOFC can measure cellular alignment of contracting CMs in lieu of endpoint assay stains. In addition, the results may further suggest that the wrinkle substrate may serve as a better biomimetic surface than the line substrate in terms of cell alignment and contractile orientation.

A critical component of the drug screening platform is its detection mechanism. With the combination of Classic + Null-Full algorithm and pOFC, it was important to demonstrate the accuracy and capability of both the OF and pOFC algorithms. The OF algorithm was specifically evaluated under several scenarios (Supplementary Information). The first scenario addressed the accuracy of the algorithm by incorporating computer generated images with ideal condition of well pre-defined deformations and movements. A few of the test images were deformed by applying a pinch or stretch filter, and the resulting motion vectors accurately depicted each of the deformations (Supplementary Fig. 4A). The test images were then moved in predetermined directions and distances within two types of backgrounds: a high contrast and a similar background. The directions of all movements

Author Manuscript Author Manuscript Author Manuscript Author Manuscript

were accurately detected by the corresponding motion vectors (Supplementary Fig. 4B). In terms of magnitude, the measured displacements of the square image were nearly identical to that of the predetermined value. However, the measured displacements for the circle images were approximately 50% of the predetermined distance. This reduction in magnitude was the result of the calculations accounting for the stationary part of the background. However, a more comparable evaluation would be to look at the ratio of the average displacements between the two sets of the circle images. The value was around 3.20 and that is comparable to the true value of 3.25.

The goal of the second scenario was to measure and compare the noise levels and movements between bright field and fluorescent bead images under the experimental conditions (Supplementary Fig. 5). Unlike computer generated images, slight fluctuations in the light source or vibrations in the setup could change the intensity and introduce noise to the captured images. For the line and wrinkle substrates, they had minimal noise; whereas, the high noise of the flat substrate could be attributed to the lack of features on the surface that can act as reference points. As a result, an aperture problem may have occurred. Even with the slightly higher noise level, the resulting motion vectors and contractile properties of hESC-CMs on flat substrates of bright field images were comparable to those of fluorescent bead images. To address the difference in noise levels, the accuracy of all contractile properties reported in the manuscript were reported as ratios between motion vectors instead of as absolute values. Therefore, unlike traction force microscopy in which the accuracy of the displacements of beads are crucial, these results further validate the feasibility of analyzing contracting cardiac cells with relatively low resolution bright field microscopy.

After evaluating each component of the system independently (biomimetic wrinkles, OF, and pOFC codes), all the components were integrated to create a platform for monitoring functional cardiac properties. To demonstrate the efficacy of this platform for cardiotoxicity screening, the effects of E-4031 and isoprenaline on cardiac cells were investigated. Both drugs were chosen due to their well-established and recorded physiological and electrophysical effects on the native heart. At the same time, the two drug components differ in their mechanism of cardiotoxicity. The goals of these experiments were to not only capture cardiotoxicity but also discern the various types of cardiotoxic mechanisms within the platform. It is known that E-4031 inhibits the rapid component (I_{Kr}) of the delayed rectifier potassium currents, and can subsequently induce long QT Syndrome and prolonged action potential duration [32]. Cardiac cells from all surfaces exhibited increased contractile duration when treated with 10 nM E-4031; however, only those grown on the wrinkles responded to 3 nM of E-4031 as indicated by reduction in the contractile orientation. The concentrations of 3 and 10 nM of E-4031 are comparable to the published IC_{50} in hERG channel assay (7 nM) [33,34]. It is important to note that the drug specifically affected only the relaxation peak. The broadened relaxation peak and the overall increased contractile duration can be interpreted as a result of a delay in repolarization. In addition, the delay in repolarization prolongs the refractory period which mitigates the reentry of arrhythmia. As a result, the contractile synchronicity for all conditions was not affected by the drug. All the findings suggest that the drug screening platform can not only detect potential cardiotoxicity but also help elucidate the mechanism in which the cardiotoxicity occurs.

Author Manuscript Author Manuscript Author Manuscript Author Manuscript

Isoprenaline is a known chronotropic, dromotropic, and inotropic agent to cardiac cells. This drug was originally developed for treating asthma; however, arrhythmia is a known serious adverse effect [35]. After administration of the drug compound, all cells exhibited increase in contractile frequency and acceleration on all surfaces regardless of cell ages (Fig. 4, table). The drug also affected the contractile duration (all three trials), synchronicity (all three trials), and orientation (trial 2 and 3 only) of cells grown on the wrinkles; these differences were not evident in the flat and line substrates. While hESC-CMs demonstrated immature properties, providing these cells with topographical cues that are similar to those in the native heart might force the cells to behave as a more mature tissue. Therefore, a more evident contractile response to the drug treatment for those grown on the wrinkles can be quantified compared to the other two surfaces.

The topographical effects on CMs could also be inferred from these sets of experiments. While most of the contractile parameters were similar between cells grown on the flat and wrinkles at differentiation day 40 and 60 (Supplementary Figs. 7 and 8), at differentiation day 20, the cells grown on the wrinkles were more responsive to the drug than those grown on both flat and line surfaces (Fig. 4, bar graphs). Since isoprenaline is known for affecting calcium ion channels, these results could imply that the expression and development of ion channels of cells grown on the wrinkles might be more effective than those grown on the other surfaces at early differentiation day. Although assays such as RT-PCR need to be performed in order to conclude such a claim, this platform has nevertheless demonstrated its usefulness not only in drug screening, but also offers interesting phenomenon potentially important in basic cardiac research.

5. Conclusions

Drug-induced cytotoxicity is a main reason for drug attrition. To increase the efficiency of drug development, and potentially minimize animal testing, we have introduced an integrated biomimetic functional cardiac monitoring platform. This platform combines a biomimetic cardiac culture wrinkled substrate as well as software to noninvasively detect contractile properties under bright field. The wrinkles are fast, easy, and inexpensive to fabricate when compared to the more traditional photolithography methods. The software is able to detect and extract cardiac contractile properties under bright field microscopy. In this manuscript, this platform was used to study the effects of E-4031 and isoprenaline on hESC-CMs, and was able to detect bradycardia and tachycardia, respectively. Furthermore, the results from the drug screen experiment also suggested there might be a cell age dependent drug behavioral difference of hESC-CMs. Overall, this platform is able to recapitulate cardiotoxicity results of E-4031 and isoprenaline, and can be easily implemented as a versatile tool in basic cardiac research and predictive toxicology.

Supplementary Material

Refer to Web version on PubMed Central for supplementary material.

Author Manuscript Author Manuscript Author Manuscript Author Manuscript

Funding sources

This work was supported in part by the California Institute for Regenerative Medicine (Grant#: RN2–00921-1), the NIH Director's New Innovator Award Program (Khine, 1DP2OD007283) and NSF (Fowlkes, DBI-1053036).

References

[1]. Kola I, Landis J. Can the pharmaceutical industry reduce attrition rates? Nat Rev Drug Discov 2004;3:711–5. [PubMed: 15286737]

[2]. Shah RR. Can pharmacogenetics help rescue drugs withdrawn from the market? Pharmacogenomics 2006;7:889–908. [PubMed: 16981848]

[3]. Booth B, Glassman R, Ma P. Oncology's trials. Nat Rev Drug Discov 2003;2: 609–10. [PubMed: 12908467]

[4]. Laflamme MA, Chen KY, Naumova AV, Muskheli V, Fugate JA, Dupras SK, et al. Cardiomyocytes derived from human embryonic stem cells in pro-survival factors enhance function of infarcted rat hearts. Nat Biotechnol 2007;25: 1015–24. [PubMed: 17721512]

[5]. Yang L, Soonpaa MH, Adler ED, Roepke TK, Kattman SJ, Kennedy M, et al. Human cardiovascular progenitor cells develop from a KDR+ embryonicstem-cell-derived population. Nature 2008;453:524–8. [PubMed: 18432194]

[6]. Zhang J, Klos M, Wilson GF, Herman AM, Lian X, Raval KK, et al. Extracellular matrix promotes highly efficient cardiac differentiation of human pluripotent stem cells: the matrix sandwich method. Circ Res 2012;111:1125–36. [PubMed: 22912385]

[7]. Mandenius CF, Steel D, Noor F, Meyer T, Heinzle E, Asp J, et al. Cardiotoxicity testing using pluripotent stem cell-derived human cardiomyocytes and state-of-the-art bioanalytics: a review. J Appl Toxicol 2011;31:191–205. [PubMed: 21328588]

[8]. Schaaf S, Shibamiya A, Mewe M, Eder A, Stohr A, Hirt MN, et al. Human engineered heart tissue as a versatile tool in basic research and preclinical toxicology. PLoS One 2011;6:e26397. [PubMed: 22028871]

[9]. Mercola M, Colas A, Willems E. Induced pluripotent stem cells in cardiovascular drug discovery. Circ Res 2013;112:534–48. [PubMed: 23371902]

[10]. Braam SR, Tertoolen L, van de Stolpe A, Meyer T, Passier R, Mummery CL. Prediction of drug-induced cardiotoxicity using human embryonic stem cell-derived cardiomyocytes. Stem Cell Res 2010;4:107–16. [PubMed: 20034863]

[11]. Song LS, Guatimosim S, Gomez-Viquez L, Sobie EA, Ziman A, Hartmann H, et al. Calcium biology of the transverse tubules in heart. Ann N Y Acad Sci 2005;1047:99–111. [PubMed: 16093488]

[12]. Passier R, Denning C, Mummery C. Cardiomyocytes from human embryonic stem cells. Handb Exp Pharmacol 2006:101–22. [PubMed: 16370326]

[13]. Engelmayr GC Jr, Cheng M, Bettinger CJ, Borenstein JT, Langer R, Freed LE. Accordion-like honeycombs for tissue engineering of cardiac anisotropy. Nat Mater 2008;7:1003–10. [PubMed: 18978786]

[14]. Kim DH, Lipke EA, Kim P, Cheong R, Thompson S, Delannoy M, et al. Nanoscale cues regulate the structure and function of macroscopic cardiac tissue constructs. Proc Natl Acad Sci U S A 2010;107:565–70. [PubMed: 20018748]

[15]. Grosberg A, Alford PW, McCain ML, Parker KK. Ensembles of engineered cardiac tissues for physiological and pharmacological study: heart on a chip. Lab Chip 2011;11:4165–73. [PubMed: 22072288]

[16]. Heidi Au HT, Cui B, Chu ZE, Veres T, Radisic M. Cell culture chips for simultaneous application of topographical and electrical cues enhance phenotype of cardiomyocytes. Lab Chip 2009;9:564–75. [PubMed: 19190792]

[17]. Bursac N, Parker KK, Iravanian S, Tung L. Cardiomyocyte cultures with controlled macroscopic anisotropy: a model for functional electrophysiological studies of cardiac muscle. Circ Res 2002;91:e45–54. [PubMed: 12480825]

Author Manuscript Author Manuscript Author Manuscript Author Manuscript

[18]. Au HT, Cheng I, Chowdhury MF, Radisic M. Interactive effects of surface topography and pulsatile electrical field stimulation on orientation and elongation of fibroblasts and cardiomyocytes. Biomaterials 2007;28:4277–93. [PubMed: 17604100]

[19]. Chen A, Lieu DK, Freschauf L, Lew V, Sharma H, Wang J, et al. Shrink-film configurable multiscale wrinkles for functional alignment of human embryonic stem cells and their cardiac derivatives. Adv Mater 2011;23:5785–91. [PubMed: 22065428]

[20]. Wang J, Chen A, Lieu DK, Karakikes I, Chen G, Keung W, et al. Engineered anisotropic monolayers of human embryonic stem cell-derived ventricular cardiomyocytes by functional alignment for enhanced safety against arrhythmias. Biomaterials. 10.1016/j.biomaterials.2013.07.039; 2013.

[21]. Peng S, Lacerda AE, Kirsch GE, Brown AM, Bruening-Wright A. The action potential and comparative pharmacology of stem cell-derived human cardiomyocytes. J Pharmacol Toxicol Methods 2010;61:277–86. [PubMed: 20153443]

[22]. Stoelzle S, Haythornthwaite A, Kettenhofen R, Kolossov E, Bohlen H, George M, et al. Automated patch clamp on mESC-derived cardiomyocytes for cardiotoxicity prediction. J Biomol Screen 2011;16:910–6. [PubMed: 21775699]

[23]. Hossain MM, Shimizu E, Saito M, Rao SR, Yamaguchi Y, Tamiya E. Non-invasive characterization of mouse embryonic stem cell derived cardiomyocytes based on the intensity variation in digital beating video. Analyst 2010;135: 1624–30. [PubMed: 20517541]

[24]. Stummann TC, Wronski M, Sobanski T, Kumpfmueller B, Hareng L, Bremer S, et al. Digital movie analysis for quantification of beating frequencies, chronotropic effects, and beating areas in cardiomyocyte cultures. Assay Drug Dev Technol 2008;6:375–85. [PubMed: 18532900]

[25]. Hayakawa T, Kunihiro T, Dowaki S, Uno H, Matsui E, Uchida M, et al. Noninvasive evaluation of contractile behavior of cardiomyocyte monolayers based on motion vector analysis. Tissue Eng Part C Methods 2012;18:21–32. [PubMed: 21851323]

[26]. Adiv G Determining three-dimensional motion and structure from optical flow generated by several moving objects. IEEE Trans Pattern Anal Mach Intell 1985;7:384–401. [PubMed: 21869277]

[27]. Sun D, Roth S, Black MJ. Secrets of optical flow estimation and their principles. Proc IEEE Comput Soc Conf Comput Vis Pattern Recognit 2010:2432.

[28]. Kita-Matsuo H, Barcova M, Prigozhina N, Salomonis N, Wei K, Jacot JG, et al. Lentiviral vectors and protocols for creation of stable hESC lines for fluorescent tracking and drug resistance selection of cardiomyocytes. PLoS One 2009;4:e5046. [PubMed: 19352491]

[29]. Feinberg AW, Alford PW, Jin H, Ripplinger CM, Werdich AA, Sheehy SP, et al. Controlling the contractile strength of engineered cardiac muscle by hierarchal tissue architecture. Biomaterials 2012;33:5732–41. [PubMed: 22594976]

[30]. Saffitz JE, Kanter HL, Green KG, Tolley TK, Beyer EC. Tissue-specific determinants of anisotropic conduction velocity in canine atrial and ventricular myocardium. Circ Res 1994;74:1065–70. [PubMed: 8187276]

[31]. Kleber AG, Rudy Y. Basic mechanisms of cardiac impulse propagation and associated arrhythmias. Physiol Rev 2004;84:431–88. [PubMed: 15044680]

[32]. Sanguinetti MC, Jurkiewicz NK. Two components of cardiac delayed rectifier K+ current. Differential sensitivity to block by class III antiarrhythmic agents. J Gen Physiol 1990;96:195–215. [PubMed: 2170562]

[33]. Zhou Z, Gong Q, Ye B, Fan Z, Makielski JC, Robertson GA, et al. Properties of HERG channels stably expressed in HEK 293 cells studied at physiological temperature. Biophys J 1998;74:230–41. [PubMed: 9449325]

[34]. Redfern WS, Carlsson L, Davis AS, Lynch WG, MacKenzie I, Palethorpe S, et al. Relationships between preclinical cardiac electrophysiology, clinical QT interval prolongation and torsade de pointes for a broad range of drugs: evidence for a provisional safety margin in drug development. Cardiovasc Res 2003;58:32–45. [PubMed: 12667944]

[35]. Waldeck B Beta-adrenoceptor agonists and asthma–100 years of development. Eur J Pharmacol 2002;445:1–12. [PubMed: 12065188]

Author Manuscript Author Manuscript Author Manuscript Author Manuscript

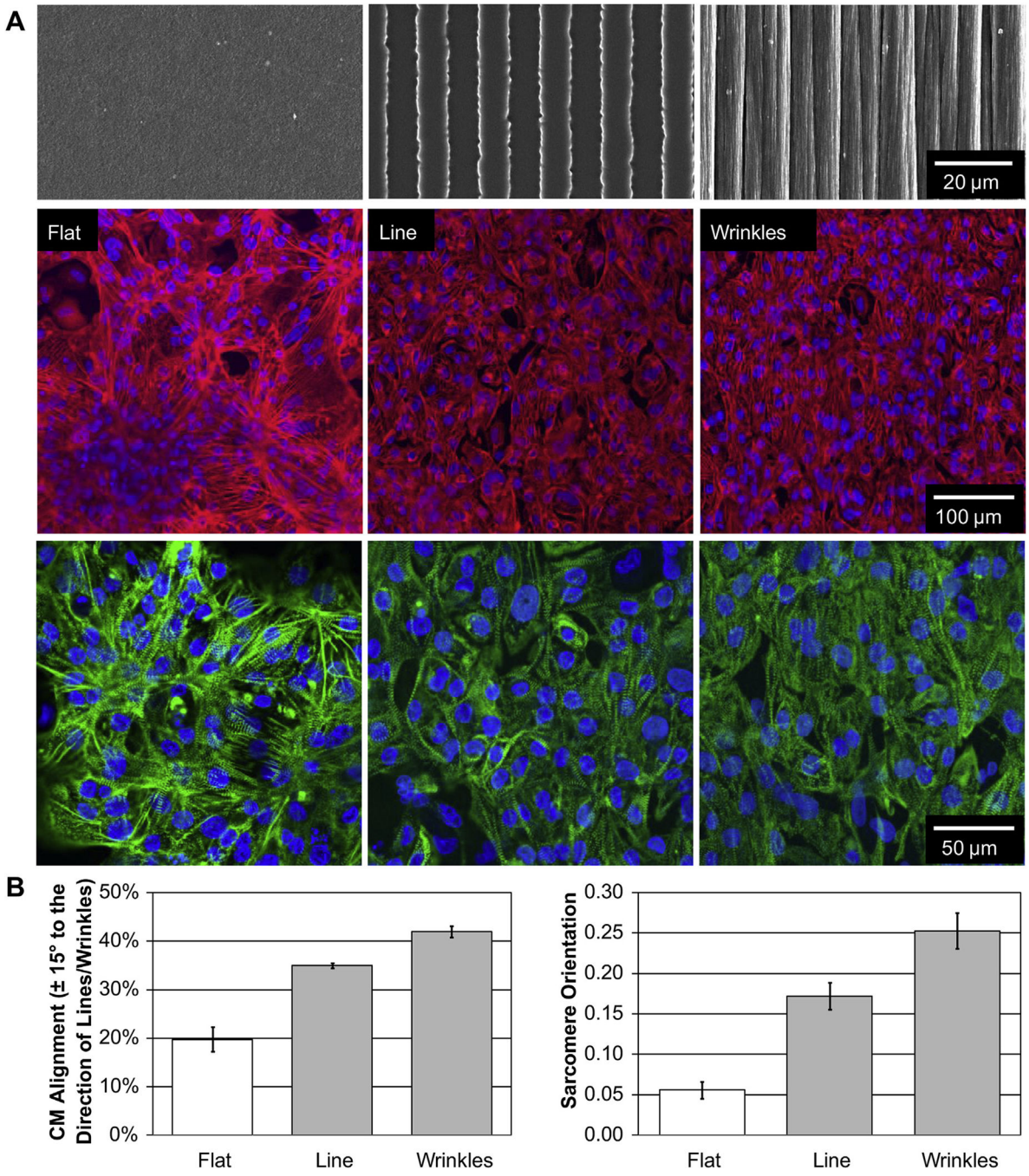

Fig. 1.

Alignment of hESC-CMs. A) (top panel) SEM images of flat, line, and wrinkled substrates at 1000x magnification. (middle panel) Fluorescent images of f-actin of hESC-CMs aligned on various topographies. The images were taken at 20x magnification. (lower panel) Fluorescent images of α-actinin of hESC-CMs aligned on various topographies. The images were taken at 40x magnification. B) (left panel) Quantification of the f-actin alignment efficiency. Bar graph showed the percent f-actin alignment. (right panel) Quantification of the sarcomere alignment efficiency using orientation organization parameter.

Author Manuscript Author Manuscript Author Manuscript Author Manuscript

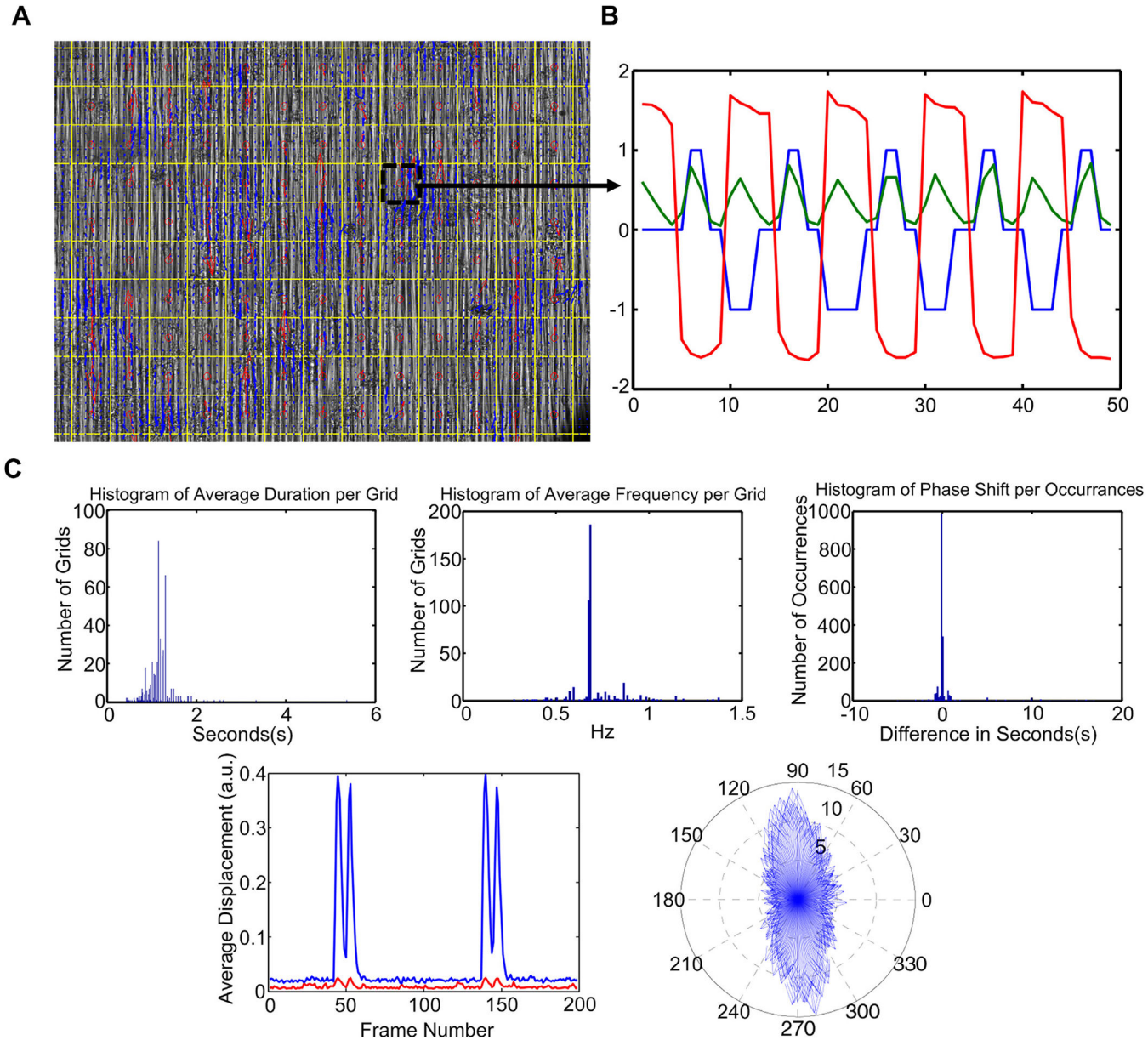

Fig. 2.

Post optical flow contraction analysis. A) Gridded (yellow boxes) image with motion vectors generated from the OF code (blue lines), and averaged motion vector for each grid (red arrows). B) Contraction analysis plot. Green line is the displacement; red line is the direction of motion vector in radians; blue line is the categorical plot. For the trace of categorical plot, a value of 1 indicates contraction, and a value of −1 indicates relaxation. *X*-axis is the frame number, and *y*-axis represents arbitrary unit, radian, and dimensionless for green, red, and blue lines, respectively. C) Sample results generated by the pOFC code including histograms of contractile duration, frequency, and synchronicity (labeled as phase shift). Contractile orientation is represented in two graphs: x- and y-motion vector traces (bottom left, blue is y, and red is x), and a compass plot (bottom right).

Author Manuscript Author Manuscript Author Manuscript Author Manuscript

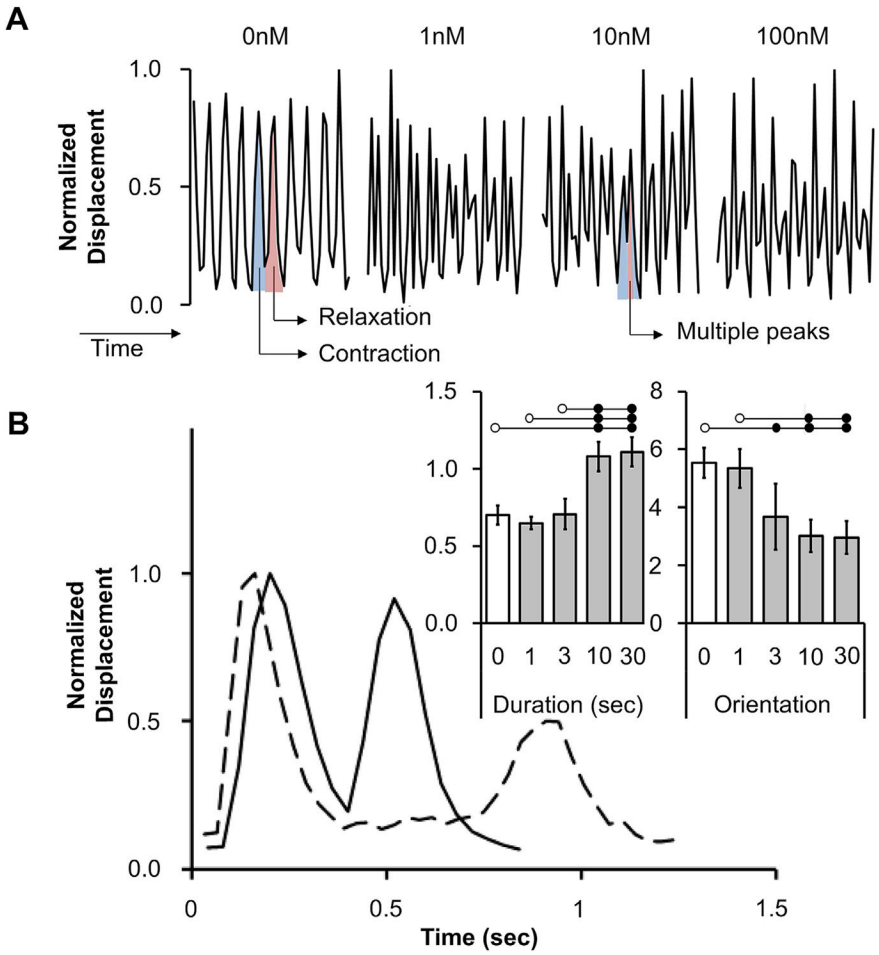

Fig. 3.

Effects of drugs on contractile displacements of cells grown on the wrinkles. A) Isoprenaline. Blue color represents contraction peak, and red color represents relaxation peak. B) E-4031. Solid line is without E-4031, and dashed line is with 30 nM of E-4031. The bar graph represents the average contractile durations and orientations for cells under 0, 1, 3, 10, and 30 nM of E-4031. The white circles and the corresponding line indicate the condition at which the rest of the conditions are compared to, and the black circles indicate the significance of the results ($p < 0.05$) from t-test. For instance, the 0 nM condition from the contractile duration is statistically different (shown by the presence of the black circles) when compared to both 10 and 30 nM.

Author Manuscript Author Manuscript Author Manuscript Author Manuscript

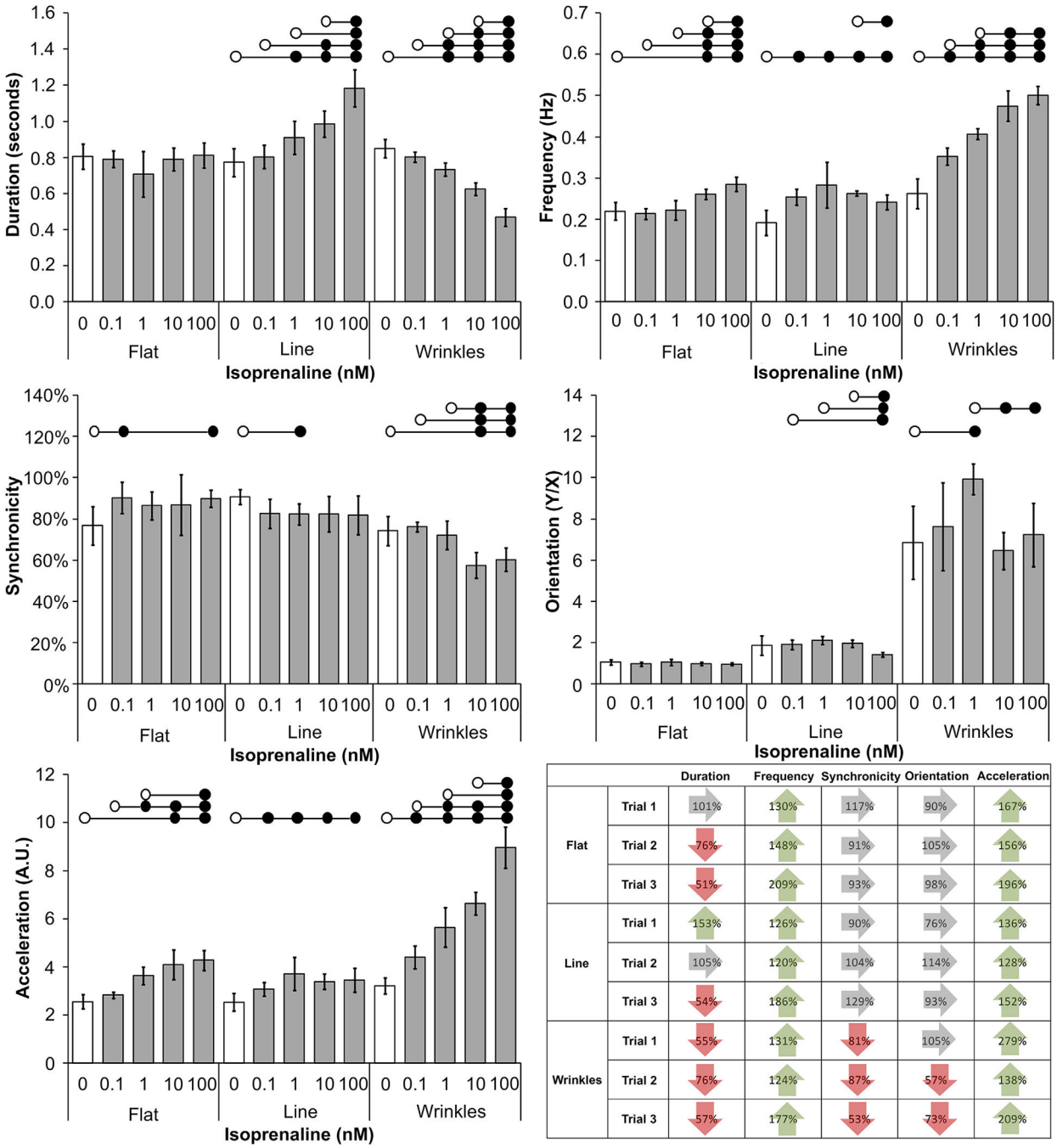

		Duration	Frequency	Synchronicity	Orientation	Acceleration
Flat	Trial 1	101%	130%	117%	90%	167%
	Trial 2	76%	148%	91%	105%	156%
	Trial 3	51%	209%	93%	98%	196%
Line	Trial 1	153%	126%	90%	76%	136%
	Trial 2	105%	120%	104%	114%	128%
	Trial 3	54%	186%	129%	93%	152%
Wrinkles	Trial 1	55%	131%	81%	105%	279%
	Trial 2	76%	124%	87%	57%	138%
	Trial 3	57%	177%	53%	73%	209%

Fig. 4.

Effects of isoprenaline on cardiac cells growing on various topographies. Bar graphs summarized results from trial 1, which evaluated the drug effects on cells at differentiation day 20. The table summarized the changes in contractile parameters between 0 and 100 nM isoprenaline in all trials. The values are the percent changes compared to the 0 nM condition. Green up arrow indicated an increase, gray horizontal arrow indicated no change,

and red down arrow indicated a decrease in the values associated with the corresponding parameters.

Author Manuscript Author Manuscript Author Manuscript Author Manuscript